ДГКС Друштво грађевинских конструктера Србије
ASES Association of Structural Engineers of Serbia
R-10
Kongres 2022
Congress 2022

Ivan Nackov[1], *Aljoša Filipović*[2], *Jelena Dobrić*[3]

NOVI PRISTUP PRORAČUNA UGAONIKA OD NERĐAJUĆEG ČELIKA – PROCENA ZASNOVANA NA NUMERIČKIM PODACIMA

Rezime:

Stubovi od ugaonika pokazuju složeno strukturno ponašanje koje proizilazi iz specifičnih geometrijskih odlika – ugaonike karakteriše mala torziona krutost i nedostatak otpornosti na savijanje, što dovodi do osetljivosti na fenomene izvijanja koji uključuju torziju. Brojne naučne studije pokazale su da su aktuelni evropski standardi za čelične konstrukcije konzervativni sa velikim rasipanjem podataka u slučaju stubova od ugaonika kod kojih do loma dolazi usled fleksiono-torzionog izvijanja. Nova proračunska procedura je razvijena na Imperijal koledžu u Londonu, koja obuhvata uticaj tranzicije u ponašanju nakon izvijanja i interaktivne efekte između fleksiono-torzionih oblika izvijanja i oblika izvijanja oko slabije ose. Ovaj rad daje procenu tačnosti ove procedure. Poređenje numeričkih podataka i njihovih proračunskih procena pokazuje dobru korelaciju, što ukazuje na bolju tačnost i doslednost u proceni nosivosti u poređenju sa postojećim kodifikovanim pravilima proračuna.

Ključne reči: nerđajući čelik, ugaonik, kritična sila, izvijanje, torziono, fleksiono, proračun.

A NEW DESIGN APPROACH FOR STAINLESS STEEL ANGLES – ACCURACY ASSESSMENT BASED ON NUMERICAL DATA

Summary:

The angle columns exhibit complex structural behaviour that arises from specific geometry features— the angle-section is characterised by low torsional stiffness and lack of primary warping resistance, leading to high sensitivity to buckling phenomena involving torsion. Numerous scientific studies have shown that the current European codes for steel structure are conservative with a high data scatter in cases of angle columns failing in flexural–torsional buckling. A novel design procedure has been developed at Imperial College in London, capturing the transition influence in post-buckling behaviour and the interactive effects between the flexural–torsional and minor-axis flexural buckling modes. This paper provides an accuracy assessment of this procedure. The comparison between the numerical data and their design estimates shows a good correlation, indicating improved accuracy and consistency in resistance predictions compared to the existing codified design rules.

Keywords: stainless steel, angle section, critical force, buckling, torsional, flexural, design.

---

[1] *Teaching assistant, Bulevar kralja Aleksandra 73 Beograd, inackov@grf.bg.ac.rs*
[2] *Assistant professor, Bulevar kralja Aleksandra 73 Beograd, afilipović@grf.bg.ac.rs*
[3] *Associate professor, Bulevar kralja Aleksandra 73 Beograd, jelena@imk.grf.bg.ac.rs*

1. INTRODUCTION

The angle columns exhibit the specific behavioural features, which are responsible for the fact that the current European codes [1], [2] for the design of steel structures do not adequately predict their ultimate responses. The equal-leg angle is singly symmetric cross-section with the shear centre located at the intersection of the leg mid-lines — this implies the lack of primary warping resistance and minute torsional stiffness, thus rendering a high susceptibility to instability phenomena involving torsion effects. The equal-leg angle columns fail in a major-axis flexural–torsional buckling (FTB) mode in the low-to-intermediate slenderness range, and a minor-axis flexural buckling (FB) mode in the high slenderness range. Besides, the clear scientific evidence corroborates that the critical buckling modes of short-to-intermediate lengths columns exhibit a length-dependent interaction between major-axis FTB and minor-axis FB representing a unique interactive instability phenomenon [3]. The short and intermediate length angle columns exhibit the mixed major-axis flexural and torsional deformations — the structural behaviour is featured by single half-wave critical buckling mode with no transverse bending of the cross-section walls (legs). This means that the critical buckling modes with several half-waves (local buckling) never occur in the angle columns. The torsional features of angle sections also depend on the leg width-to-thickness ratio; by increasing the leg widths, the distance between the shear centre and the section centroid is also increase, thus leading to FTB failure in the entire overall column slenderness range.

As an example, the nominal geometric properties of the thin-walled equal-leg angle-section 100 × 4 mm are shown in Table 1. By using the computer program CUFSM [4] and yield strength f_y=527 N/mm^2, the elastic torsional-flexural buckling stress for a nominal equal-leg angle section under compression was found to be 116.3 N/mm^2, with a corresponding half-wavelength of 2500 mm, see Figure 1.

Table 1 – Nominal geometry properties of an equal-leg angle section 100 × 4 mm.

Angle	A (mm^2)	I_y (mm^4)	I_z (mm^4)	I_u (mm^4)	I_v (mm^4)	J (mm^6)	I_w (mm^6)
100 × 4	766.4	772039.3	772039.3	1254695.9	289382.8	4087.6	81262.1
A − the gross cross-sectional area; I_y, I_z, I_u and I_v – the second moment of area about geometric and principal axes, respectively; J – the St.-Venant torsion constant; I_w – secondary warping constant.							

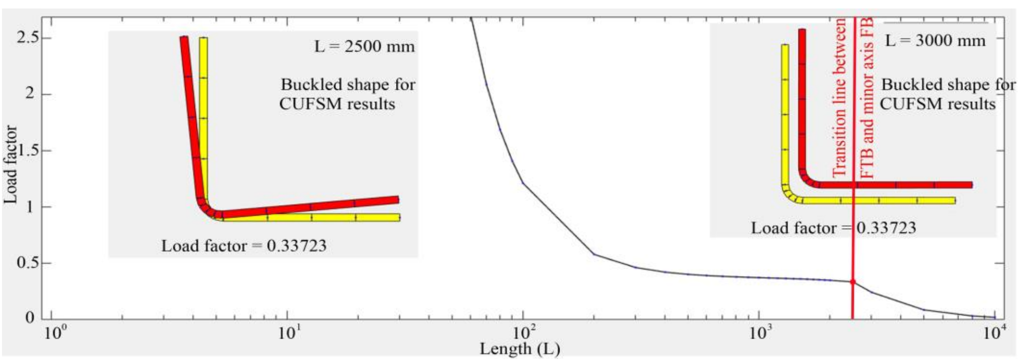

Figure 1 - Elastic critical buckling load factor versus column length curve for the equal-leg angle 100 × 4 mm.

In view of what was previously mentioned, the rational structural model for design of equal-leg angle column should be based on the torsional buckling (TB), instead of local buckling (LB) behaviour. The numerous scientific investigations [5], [6], [7], [8] have demonstrated that existing design procedures stated in the European design codes EN 1993-1-1 [1] and EN 1993-1-4 [2] are generally conservative in predicting the ultimate resistances of equal-angle columns. It is worth noting that the EN 1993 design approach is based on a couple of conceptual shortcomings influencing the inaccuracy in predicting the failure loads of these columns failing in FTB — it does not use the interaction between major-axis FTB and minor-axis FB (columns with both slender and non-slender angle-sections) and views LB and FTB as two different phenomena, thus considering in the calculations the same instability effect twice (columns with slender angle-sections). This issue was emphasized in research of Behzadi-Sofiani et al. [8], addressing fixed-ended carbon steel and stainless steel equal-leg angle columns. The authors demonstrate that TB and LB are essentially two names of the same phenomenon, confirming in this way the evidence reported in [9], where it is shown that these instabilities can only occur in longitudinally restrained angle columns.

The paper presents the results of a nonlinear finite element (FE) parametric study covering fixed-ended cold-formed stainless steel (CFSS) equal-leg angle columns failing in major-axis FTB and minor-axis FB. A wide range of cross-section slenderness and column lengths produced from austenitic, duplex and ferritic stainless steel grades were considered. The parametric study was based on the FE models that were calibrated and validated against the experimental results reported in [10]. The FE column ultimate resistances were employed to perform independent accuracy assessment of the novel procedure proposed for design of stainless steel equal-leg angle columns, which was developed and validated in [8]. The statistical indicators concerning the failure loads, are also provided, showing the quality and reliability levels of the proposed method.

2. A NEW DESIGN PROCEDURE [8]

In the low and intermediate slenderness domain, where FTB is the dominant failure mode and $N_{\mathrm{cr,TF}}/N_{\mathrm{cr,F,v}} \leqslant 1.0$, the design buckling resistance $N_{\mathrm{b,Rd}}$ of CFSS equal-leg angle section columns is given as follows:

$$N_{\mathrm{b,Rd}} = \chi_{\mathrm{TF}} A f_{\mathrm{y}} / \gamma_{\mathrm{M1}} \tag{1}$$

In the Eq. (1) the gross cross-sectional area should be used for all classes of angle-sections to avoid double-accounting of local and torsional buckling. The reduction factor χ_{TF} is given by:

$$\chi_{\mathrm{TF}} = \chi_{\mathrm{F}} + \Delta_{\mathrm{F}}(\chi_{\mathrm{T}} - \chi_{\mathrm{F}}) \tag{2}$$

The torsional buckling reduction factor χ_{T} and the flexural buckling reduction factor χ_{F} are respectively given as follow:

$$\chi_{\mathrm{T}} = \bar{\lambda}_{\mathrm{TF}} - 0.188/\bar{\lambda}_{\mathrm{TF}}^{2} \;\text{ but } \chi_{\mathrm{T}} \leqslant 1.0 \tag{3}$$

$$\chi_{\mathrm{F}} = 1/\left(\phi + \sqrt{\phi^{2} - \bar{\lambda}_{\mathrm{TF}}^{2}}\right) \;\text{ but } \chi_{\mathrm{F}} \leqslant 1.0 \tag{4}$$

and Δ_{F} is given thus:

$$\Delta_{\mathrm{F}} = \left(1 - N_{\mathrm{cr,TF}}/N_{\mathrm{cr,F,v}}\right)^{p} \tag{5}$$

where:

$$p=\begin{cases}2.0\bar{\lambda}_{\mathrm{TF}} \text{ for } \bar{\lambda}_{\mathrm{TF}} \leqslant 2.0\\ 2.93\bar{\lambda}_{\mathrm{TF}}^{0.45} \text{ for } \bar{\lambda}_{\mathrm{TF}} > 2.0\end{cases} \tag{6}$$

The torsional-flexural slenderness $\bar{\lambda}_{\mathrm{TF}}$ and parameter ϕ are given by:

$$\bar{\lambda}_{\mathrm{TF}}=\sqrt{Af_{\mathrm{y}}/N_{\mathrm{cr,TF}}} \tag{7}$$

$$\phi=0.5\left[1+\alpha\beta\left(\bar{\lambda}_{\mathrm{TF}}-\bar{\lambda}_0\right)^{\beta}+\bar{\lambda}_{\mathrm{TF}}^2\right] \tag{8}$$

For CFSS angles, the proposed values for β and the limiting slenderness $\bar{\lambda}_0$ are 1.45 and 0.2, respectively, whereas for the imperfection factor α, value of 0.49 is recommended. In the high slenderness domain where $N_{\mathrm{cr,TF}}/N_{\mathrm{cr,F,v}} > 1.0$, the design buckling resistance $N_{\mathrm{b,Rd}}$ of CFSS equal-leg angle columns should be obtained as follows:

$$N_{\mathrm{b,Rd}}=\chi_{\mathrm{F}}Af_{\mathrm{y}}/\gamma_{\mathrm{M1}} \tag{9}$$

$$\chi_{\mathrm{F}}=1/(\phi+\sqrt{\phi^2-\bar{\lambda}^2}) \text{ but } \chi_{\mathrm{F}} \leqslant 1.0 \tag{10}$$

$$\bar{\lambda}=\sqrt{Af_{\mathrm{y}}/N_{\mathrm{cr,F,v}}} \tag{11}$$

$$\phi=0.5\left[1+\eta+\bar{\lambda}^2\right] \tag{12}$$

$$\eta=\alpha\beta\left(\bar{\lambda}-\bar{\lambda}_0\right)^{\beta} \tag{13}$$

with β being a factor allowing for the influence of interactive buckling:

$$\beta=1.9-0.45N_{\mathrm{cr,TF}}/N_{\mathrm{cr,F,v}} \text{ but } 1.0 \leq \beta \leq 1.45 \tag{14}$$

When minor-axis FB is critical failure mode, the gross cross-sectional area A in Eq. (9) should be replaced by the effective area A_{eff} for columns with slender Class 4 cross-sections, since the issue of double-counting the torsional effects is no longer relevant. The imperfection factor and limiting slenderness remain as specified above, α = 0.49 and $\bar{\lambda}_0=0.2$.

3. NUMERICAL PARAMETRIC STUDY

The numerical parametric study was performed on CFSS equal-leg angle columns using the ABAQUS FE software package [11]. The linear bifurcation analysis (LBA), and geometrically and materially non-linear analysis with imperfections (GMNIA) were performed for each FE angle column. The GMNIA was developed as quasi-static with the dynamic explicit solver, and the variable non-uniform mass scaling technique of $5\text{x}10^{-6}s$ was used to shorten the computational time. In total, 14 different equal-leg angle section dimensions were considered, as in [5], providing both slender and non-slender cross-sectional behaviour. A 4-noded shell element S4R was employed to model the nominal geometry of the FE columns. A square mesh size of approximately 4 mm was chosen to discretise the flat and corner parts of the modelled cold-formed angle sections. To nonlinear material responses for austenitic, ferritic and duplex grade were replicated using the modified Ramberg-Osgood analytical model [12], as it was described in [5]. Fixed-ended boundary conditions were modelled by restraining the necessary degrees of freedom at the reference points set at the end cross-sections. By employing kinematic coupling constraints, warping was also prevented at both ends. The failure loading was applied as controlled nodal displacement at one end through a reference point that was free to move longitudinally. Initial geometric imperfections include bow imperfections (out-of-straightness), twist imperfections and cross-section imperfections (out-of-flatness of a section angle legs). A single initial twist imperfection was considered to trigger local and torsional-flexural modes: a sinusoidal half wave mode shape over the column length, reflecting twist eigenmode shape, with an amplitude of $\tan^{-1}(L/1000b)$ at the column mid-height [7], [8]. The amplitude of $L/1000$ was adopted about both principal axes for the initial out-of-straightness. The geometric imperfection pattern reflects the eigenmode displacements obtained via LBA.

4. ACCURACY ASSESSMENT OF THE NEW DESIGN PROCEDURE [8]

A comparison of the generated FE data with the design data obtained according to the proposed design procedure [8] for fixed-ended CFSS equal-leg angle columns is presented in this section. The FE parametric study comprised 156 FE columns (see Table 2), covering the slenderness range from 0.5 to 2.5, made of austenitic, ferritic and duplex grades. The numerical failure mode governed by major-axis FTB or minor-axis FB (see Figure 2) was selected to evaluate the corresponding design failure load. In the predictions of the ultimate column resistances, the safety factor was used equal to 1.0. The elastic critical buckling loads for TB, major-axis FTB and minor-axis FB were analytically determined according to the Theory of elastic stability [13] and via LBA. For analytically determined critical buckling loads, the effective buckling lengths for TB and FTB were taken to be equal to the column length L, whereas the effective buckling length for minor-axis FB was taken as $0.5L$. Figure 3 shows the comparisons between analytically and numerically obtained elastic critical buckling loads.

Table 2 – Cross-section geometries and lengths of CFSS angle columns included in the study.

Equal-leg angle section	Column length L (mm)	Leg width b (mm)	Thickness t (mm)	Internal radius r_i (mm)
50 x 50 x 2	300-2200	50	2	4
50 x 50 x 4	300-2600	50	4	8
50 x 50 x 5	300-2800	50	5	10
60 x 60 x 2	400-2400	60	2	4
60 x 60 x 4	300-3000	60	4	8
60 x 60 x 6	400-3000	60	6	12
80 x 80 x 4	300-3200	80	4	12
80 x 80 x 6	500-3200	80	6	12
150 x 150 x 4	900-3000	150	4	8
150 x 150 x 6	800-3800	150	6	12
150 x 150 x 8	600-4000	150	8	16
200 x 200 x 6	900-3300	200	6	12
200 x 200 x 8	900-3300	200	8	16

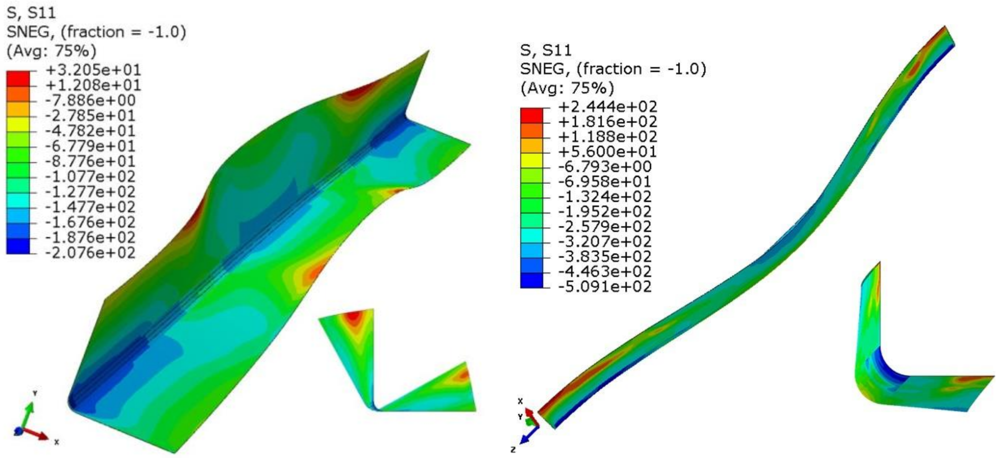

(*a*) *major-axis FTB mode of intermediate length column*

(*b*) *minor-axis FB mode of long length column*

Figure 2 - The buckling failure modes of FE CFSS equal-leg angle column.

A summary of the comparisons of the FE column compressive capacities against the resistance predictions according to the new proposal is shown in the graphs in Figures 4, 5 and 6 for austenitic, ferritic and duplex CFSS equal-leg columns, respectively, using different colour coding for each stainless steel family. The statistical indicators, mean values, standard deviation, Coefficient of Variations (CoVs) and maximum / minimum values, concerning the failure loads are also provided.

The observation of the buckling results prompts the following remarks:

- The ultimate buckling load decreases monotonically with the column length; the torsional mode almost always plays a key role: it participates in the critical buckling modes of all but the very long columns. In the low and intermediate slenderness range (approximately up to $\bar{\lambda} \approx 1.0$) columns buckle in in mixed major FTB, whereas the long length columns buckle in pure minor-axis FB.
- The well-known theoretical formula for elastic critical FTB loads [13] offers a lower prediction accuracy with a larger scatter, compared to the case of a pure minor-axis FB (see Figure 3), thus causing the prediction inaccuracy for the ultimate column capacities according to design approaches based on separated models for FTB and FB.
- In general, the proposed design approach [8], which captures the transition influence in post-buckling regime and the interactive effects between the TFB and minor-axis FB, yields safe and accurate predictions of the ultimate column strengths, especially in the case of CFSS angle columns that failed dominantly by FB. The assessment of the design methods shows better consistency for ferritic grade, whereas a large margin with highest data scatter was found for duplex stainless steel. Also, there are fewer predictions on the unsafe side for austenitic grade.

- Using the results of previous investigations, collected from literature [5], [6], [8], the comparisons presented herein for FTB modes, indicate an improvement in resistance predictions relative to that currently given in EN 1993. Again, the highest accuracy and consistency of capacity predictions were found for ferritic grade, whereas there is greater scatter in the data with a few uncertain predictions for the austenitic and duplex grades.

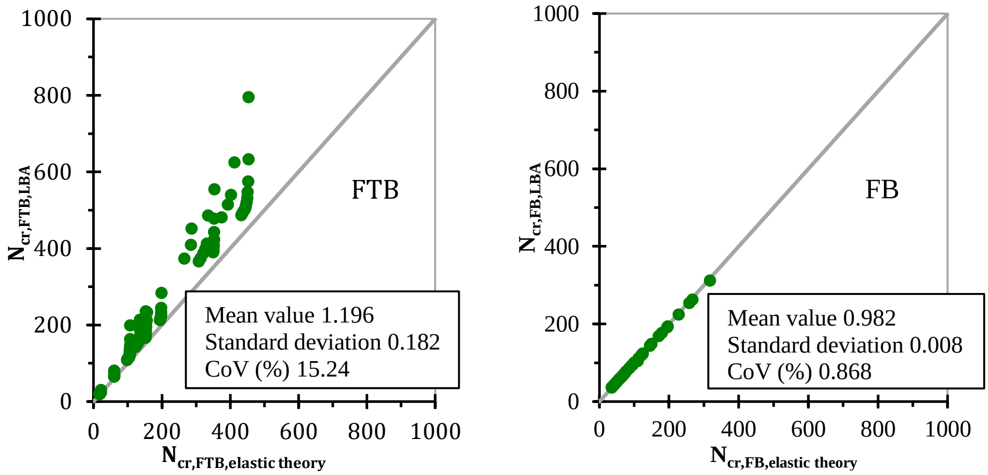

(*a*) *major-axis FTB mode* (*b*) *minor-axis FB mode*

Figure 3 - Comparisons between analytically and numerically obtained elastic critical buckling loads.

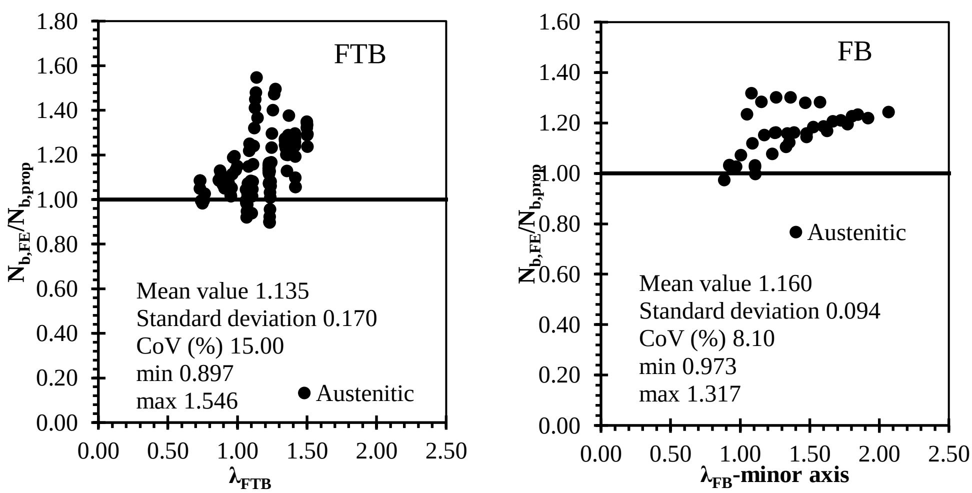

(*a*) *major-axis FTB mode* (*b*) *minor-axis FB mode*

Figure 4 - FE results against the new design proposal for the austenitic CFSS angle columns.

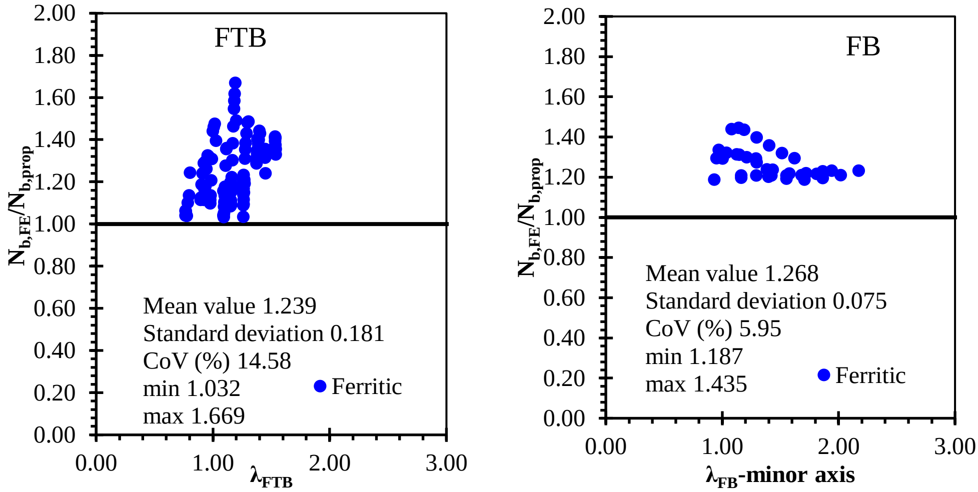

(*a*) *major-axis FTB mode* (*b*) *minor-axis FB mode*

Figure 5 - FE results against the new design proposal for the ferritic CFSS angle columns.

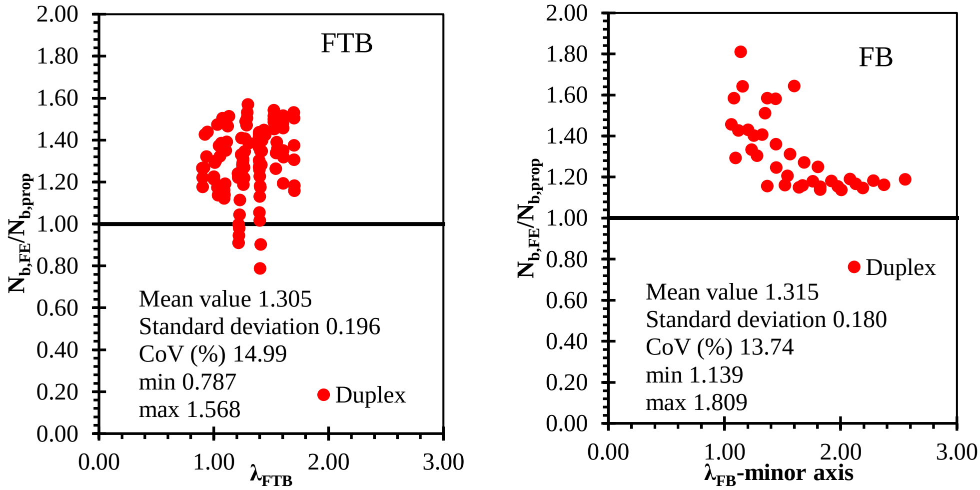

(*a*) *major-axis FTB mode* (*b*) *minor-axis FB mode*

Figure 6 - FE results against the new design proposal for the duplex CFSS angle columns.

5. CONCLUSIONS

This paper presents the accuracy assessment of the new design proposal for CFSS equal-leg angle columns failing by major-axis FTB and minor-axis FB, using FE database. The FE parametric study covers the slenderness range from 0.5 to 2.5 of 156 FE columns produced from austenitic, ferritic and duplex grades. The results of the comparative study showed that the statistical indicators and data trend lines obtained herein are similar to those acquired in the research of Behzadi-Sofiani et al. [8] — the novel design proposal provides notable improvements in both the accuracy and consistency of column ultimate resistance predictions.

REFERENCES

[1] Eurocode 3: Design of steel structures – Part 1-1: General rules and rules for buildings EN 1993-1-1, Brussels, Belgium, CEN 2005.

[2] Eurocode 3: Design of steel structures – part 1-4: General rules – supplementary rules for stainless steels, including amendment A1 (2015), EN 1993-1-4:2006+A1:2015, Brussels, Belgium, CEN 2015.

[3] A. Landesmann, D. Camotim, P.B. Dinis, R. Cruz, Short-to-intermediate slender pinended cold-formed steel equal-leg angle columns: experimental investigation, numerical simulations and DSM design, Eng. Struct., 132 (2017) 471–93.

[4] Schafer BW, Ádány S. Buckling analysis of cold-formed steel members using CUFSM: conventional and constrained finite strip methods. In: Proceedings of the eighteenth international speciality conference on cold-formed steel structures. Orlando (USA); 2006.

[5] Dobrić J, Filipović A, Baddoo N, Marković Z, Buđevac D. Design procedures for cold-formed stainless steel equal-leg angle columns, Thin-Walled Structures, 159 (107210), 2020, pp.19.

[6] Dobrić J, Filipović A, Baddoo N, Buđevac D, Rossi B. Design criteria for pin-ended hot-rolled and laser-welded stainless steel equal-leg angle columns, Thin-Walled Structures, 167(108175), 2021, pp. 24.

[7] Behzadi-Sofiani B, Gardner L, Ahmer Wadee M, Dinis P.B, Camotim D. Behaviour and design of fixed-ended steel equal-leg angle section columns, Journal of Constructional Steel Research 182 (2021) 106649, pp 14.

[8] Behzadi-Sofiani B, Gardner L, Ahmer Wadee M. Stability and design of fixed-ended stainless steel equal-leg angle section compression members, Engineering Structures 249 (2021) 113281, pp 17.

[9] P.B. Dinis, D. Camotim, N. Silvestre, On the mechanics of thin-walled angle column instability, Thin-Walled Structures 52 (2012) 80-89.

[10] J. Dobrić, A. Filipović, Z. Marković, N. Baddoo, Structural response to experimental axial testing of cold-formed stainless steel equal angle columns, Thin-Walled Struct., 156 (2020) 1-16.

[11] ABAQUS User Manual. Version 6.12. Providence, RI, USA: DS SIMULIA Corp; 2012.

[12] I. Arrayago, E. Real, L. Gardner, Description of stress-strain curves for stainless steel alloys, Materials and Design, 87 (2015) 540-552.

[13] S.P. Timoshenko, J.M. Gere, Theory of Elastic Stability, 2nd ed. McGraw-Hill Book Company, Inc., New York, USA, 1961.